Effects and mechanisms of AMIGO2 in proliferation, migration and drug resistance of bladder cancer

Dali Han
Lanzhou University Second Hospital
Bin Xiong
Lanzhou University Second Hospital
Xiangxiang Zhang
Lanzhou University Second Hospital
Chaohu Chen
Lanzhou University Second Hospital
Zhiqiang Yao
Lanzhou University Second Hospital
Hao Wu
Lanzhou University Second Hospital
Jinlong Cao
Lanzhou University Second Hospital
Jianpeng Li
Lanzhou University Second Hospital
Pan Li
Lanzhou University Second Hospital
Zhiping Wang
Lanzhou University Second Hospital
Jun-Qiang Tian (ery_tianjq@lzu.edu.cn)
Lanzhou University Second Hospital

Research

Keywords: AMIGO2, Bladder cancer, Proliferation, Bioinformatics

Posted Date: June 10th, 2020

DOI: https://doi.org/10.21203/rs.3.rs-34249/v1

Abstract

Background Bladder cancer is the most common malignancy in urinary system, but the therapeutic targets remain elusive. This study aims to reveal the relationship between AMIGO2 and proliferation, migration, drug-resistance and tumorigenicity of bladder cancer, and explore the potential molecular mechanisms.

Methods The expression of AMIGO2 in human bladder cancer tissues is measured by qRT-PCR and immunohistochemistry (IHC). Stable AMIGO2 knockdown cell lines T24 and 5637 were established by lentivirus transfection. Cell viability assay (CCK-8 assay) was used to determine cell proliferation, flow cytometry analysis was utilized to detect cell cycle, and wound healing assay was proceeded to test migration ability of bladder cancer cells. Chemosensitivity to cisplatin was measured by CCK-8 assay. Xenograft mouse model was established for investigating the effect of AMIGO2 on tumor formation in vivo. The RNA Sequencing technology was used to explore differentially expressed genes (DEGs) between knockdown group and negative control group of T24. Bioinformatics analysis upon the results of RNA-Seq was proceeded to understand underlying mechanisms.

Results AMIGO2 was upregulated in bladder cancer cells and tissues. Inhibited expression of AMIGO2 suppresses cell proliferation and migration, which might be mediated by cell cycle arrest in G1 phase. AMIGO2 could reduce chemoresistance to cisplatin in bladder cancer cells. Low AMIGO2 expression inhibited tumorigenicity of T24 in nude mice. 917 DEGs were identified by RNA-Sequencing technology and bioinformatics analysis. The DEGs were mainly enriched in cell-cell adhesion, ATP-binding cassette transporters (ABC transporters), PPAR signaling pathway and some other pathways. Among ten hub genes, four of them might be associated with the prognosis of bladder cancer patients.

Conclusion AMIGO2 is overexpressed in bladder cancer cells and tissues and serves as an oncogene in bladder cancer. It also reduces chemoresistance to cisplatin. The process might be regulated by particular pathways including ABC transporters and PPAR signaling pathway. Four hub genes might be associated with prognosis of bladder cancer patients.

Background

Bladder cancer (BCa) remains to be the most common malignancy in urinary system. New cases diagnosed with bladder cancer is about 549393 of all sites, number of death is about 199922, making it the 6th most common cancer in male (4.5% of all cancers) and the 10th most common cancer in both sex (3.0% of all)[1]. Urothelial carcinoma of the bladder is a common malignancy that causes approximately 150,000 deaths every year worldwide[2]. Thus, exploring more treatment options is of utmost importance. Novel approaches are emerging, including cancer vaccines, nanoparticle-based therapy, hyperthermia, cytotoxic agent, targeted therapy, immune modulators and gene therapy[3]. Among all the therapies, gene therapy remains a potential one.

Adhesion molecule with Ig-like domain 2 (AMIGO2) locates in the 12th chromosome. Chromosome region: q13.11, length: 3175bp. AMIGO2 is broadly expressed in several normal human organs and tissues, including gall bladder, bladder, and 23 other tissues[4]. The protein AMIGO2 codes is an amphoteric inducing protein, whose extracellular domain has 6 leucine repeat sequences (LRR), and coated with an Ig-like domain[5]. AMIGO2 plays an essential role in tumor growth, cell adhesion and migration through collagen of gastric cancer cells[6]. In addition, AMIGO2 was required for melanoma cell proliferation and survival, which is induced by the acquisition of active cis DNA regulatory elements absent in NHMs[7].

In the present study, we explored the expression and biological functions of AMIGO2 in bladder cancer. Our study proved that AMIGO2 could promote the proliferation, migration and tumorigenicity of BCa cells. Also, we used RNA-Sequencing technology to identify the DEGs. After bioinformatics analysis, we screened the key genes and pathways, which deepened our understanding of the molecular mechanisms underlying the progression of bladder cancer. These results might hold promise for finding potential therapeutic targets of bladder cancer.

Materials And Methods

Cell culture and tissue specimen collection

The human BCa cell lines T24 and 5637 were obtained from Chinese Academy of Science, authenticated by STR profiling and tested for mycoplasma contamination. Cells were cultured in RPMI-1640 medium (Gibco, Thermo Fisher Scientific, USA), supplemented with 10% fetal bovine serum (Pan Biotech, Germany), penicillin and streptomycin (100 IU/ml). All the cells were incubated at 37℃ under a humidified atmosphere with 5% CO_2.

Bladder cancer tissues and matched adjacent non-tumor bladder tissues were collected from patients underwent radical cystectomy and pathologically diagnosed with bladder cancer at the Department of Urology, the Second Hospital of Lanzhou University. All the samples were originated as urothelial cancer, and were taken immediately after surgery and stored at -80℃ for further use. None of the patients underwent chemotherapy, radiotherapy or adjuvant treatment before surgery. All tissue samples were obtained from patients who have signed informed consent. This project was approved by the Institutional Research Ethics Committee of the Second Hospital of Lanzhou University (Approval No. 2019A-199).

Immunohistochemiscal analysis

This experiment was conducted as previously described[8]. Paraffin sections were first deparaffinized in xylene and rehydrated in graded alcohol. For antigen retrieval, the tissue slides were immersed in 0.01M citrate buffer for 2min. The endogenous peroxidase was inactivated with 3% hydrogen peroxide methanol solution and incubated in a humidified chamber with AMIGO2 antibody (1:500, Santa Cruz, USA)

overnight at 4℃. The slides were then incubated with biotinylated anti-goat IgG secondary antibody for 15min at room temperature. Sections were subsequently stained with 3, 3`-diaminobenzidine (DAB), counterstained with hematoxylin (Solarbio, Peking, China).

Cell transfection

Plasmids carrying either AMIGO2 shRNA or negative control shRNA were constructed. Lentivirus was generated in HEK-293 cells. The plasmid containing AMIGO2 cDNA was obtained from Shanghai Genechem Co., LTD. Lentivirus plasmid constructed with scramble sequence was used as control. The transfection was conducted according to the manufacturer's instructions. 1.0μg/ml of puromycin was added for screening. The cell clones stably expressing knockdown AMIGO2 and negative control were selected and expanded.

RNA extraction, reverse transcription and quantitative real-time PCR

Total RNAs were extracted from cultured cells using Tirol Reagent (Takara, Japan) according to the manufacturer's instructions. Conversion to cDNA was achieved through cDNA PrimeScript™ RT Master Mix (Perfect Real Time) (TAKARA, Japan) in reverse transcription PCR instrument (Bio-Rad Laboratories, USA). qRT–PCR was carried out using the CFX Real-Time PCR System (Bio-Rad Laboratories, USA) in a 15-μl reaction volume containing first-strand cDNA, TB Green™ Premix Ex Taq™ II (Tli RNaseH Pluse). The relative expression was calculated using the $2^{-\Delta\Delta Ct}$ method[9]. The transcription level of GAPDH was used as an internal control. The following primers were used:

AMIGO2 forward: 5'-CCTGGGAACCTTTTCAGACTG-3';

AMIGO2 reverse: 5'-GCAAACGATACTGGAATCCACT-3';

GAPDH forward: 5'-TGACTTCAACAGCGACACCCA-3';

GAPDH reverse: 5'-CACCCTGTTGCTGTAGCCAAA-3'.

Protein extraction and Western Blot

Cells were thawed on ice by ultrasonication in RIPA buffer (Beyotime, China). The resulting homogenates were centrifuged at 4℃, 12000g, for 15min, followed by the collection of the supernatants. Protein concentration was measured by BCA Protein Assay Kit (Beyotime, China). Protein isolates were then resolved on SDS-PAGE gel and transferred to polyvinylidene difluoride (PVDF) membranes (Millipore, USA). The membranes were blocked with 5% milk, incubated overnight with the primary antibodies: Anti-

AMIGO2 (Santa-Cruz, USA); Anti-GAPDH (Santa-Cruz, USA), and probed with horseradish peroxidase-conjugated secondary antibody: Anti-Mouse IgG (Santa-Cruz, USA). The blots were then detected using Pierce™ ECL Western Blotting Substrate Kit (Thermo, USA).

Flow cytometric cell cycle analysis

Cells (1×10^6) were harvested, re-suspended in PBS, fixed in 75% ice-cold ethanol, and incubated in propidium iodide (PI, 20μg/ml; Sigma, USA) in the dark for 20min. Cell cycle analysis was performed using the BD LSRII Flow Cytometry System with FACSDiva software (BD Bioscience, Franklin Lakes, USA). The data were analyzed using the Modfit LT software.

CCK-8

Cells were seeded into 96-well plates at 2000 cells/well. Cell proliferation was detected using the Cell Counting Kit-8 (CCK-8, Dojindo Laboratories, Japan). At indicated time point, CCK-8 solution was added to each well and incubated for 3h. The absorbance was determined at 450nm using a microplate reader (Tecan infinite, Switzerland).

Wound-healing assay

3×10^5 T24 or 5637 cells were seeded into 6-well plates with complete culture medium. The confluent monolayer of both cells was scratched with a 1 ml pipette tip. The cells were then washed with PBS three times and kept in the 1640 (supplemented with 10% FBS) for 48h. The wound width was recorded at 0h and 24h under a microscope.

Chemosensitivity assay

Cells were treated with different concentrations of cisplatin (0, 2, 4, 8 and 16μM, Sigma, USA) for 24h. Afterward, cell viability was measured by CCK-8 assay (Dojindo, Kumamoto, Japan) according to the manufacturer's instructions. For calculation of IC50 (half inhibition concentration), data were fitted in GraphPad Prism5 (GraphPad Software Inc., San Diego, CA, USA). The dose-response curve was plotted using the equation log (inhibitor) vs. response Variable slope. Y=Bottom + (Top-Bottom)/(1 + 10ˆ((Log IC50-X)* HillSlope))[10].

Xenograft mouse model

Nude mice (BALB/c-nu, female, 4 weeks) were bred and housed in AAALAC-accredited specific pathogen-free rodent facilities. Mice were housed in sterilized, ventilated microisolator cages and supplied with autoclaved commercial chow and sterile water. The mice were randomly divided into two groups (n=8). Tumorigenicity was determined by subcutaneously injection of T24 cells into the flanks of female nude mice (1×10^6 cells per site). The tumor size was measured 2~3 times per week, up to 28d. Tumor volumes were calculated using the following formula: $V=\pi/6$ x largest diameter x smallest diameter^2 [11]. No blinding was done. All mouse experiments were conducted with standard operating procedures approved by the University Committee on the Use and Care of Animals at the second hospital of Lanzhou University (Approval No. D2019-171).

RNA-Seq data analysis

Total RNAs of shAMIGO2 and shCtrl were extracted. We used RNA sequencing technology (Novogene, China) to identify DEGs. Briefly, the RNA-seq raw fastq data were first trimmed using Trimmomatic (V0.35). The trimmed reads were aligned to the human reference genome (NCBI GRCh38) with TopHat V2.0.12 with default parameter settings. The aligned bam files were then processed using Cufflinks V2.2.1 for gene quantification. Reads were then mapped to ERCC transcripts and quantified using TopHat V2.0.12 and Cufflinks V2.1.1 with default parameter settings. Genes with FPKM ≥ 1 in all samples were used for DEG analysis. We could upload the data from RNA-Seq to a public repository if necessary.

Data analysis and DEGs identification

The sequencing data set was normalized and analyzed using the DESeq package (1.10.1). The criteria of a false discovery ratio (FDR) <0.01 and |logFC| >2 were set as the threshold. Visualization of the volcano plot and heat map were done using R software. The most upregulated 100 genes and downregulated 100 genes were chosen for the heat map.

Biological function and pathway enrichment analysis

Through calculating the corresponding topological overlap, genes positively associated with AMIGO2 were found out and subjected to gene ontology (GO) analysis (GOSeq, Release2.12) to determine clusters of DEGs with enriched molecular functions. Kyoto encyclopedia of genes and genomes (KEGG) pathway analysis was performed via the “clusterProfiler” package in R/Bioconductor software to acquire the enriched biological process and KEGG pathway. $p<0.05$ and counts ≥ 4 were considered significant.

Module analysis of protein-protein interaction (PPI) network

Search Tool for the Retrieval of Interacting Genes (STRING) database (http://www.string- db.org/) was used to acquire PPI information for the DEGs. Cytoscape software (3.7.2) was applied to visualize the PPI network. The top DEGs with a high degree of connectivity in the PPI network were selected to discuss their function and effect on bladder cancer.

GSEA of DEGs on the whole gene expression level

Gene set enrichment analysis (GSEA) online tool (http://software.broadinstitute.org/gsea/index.jsp)[12] was applied to verify the results of GO and KEGG analysis. The cut-off criteria for GSEA were $p<0.05$. We created a chip expression profile file and a sample data file, and imported them into GSEA software. After choosing gene sets database and corresponding chip platform, setting other parameters as default, we could run GSEA and acquire pathway enrichment results on the total gene expression level.

Statistical analysis

All data were reported as mean ± SEM from three independent experiments. The two-tailed Student's t-test was used to evaluate statistical differences between two groups. The survival curve was described by the Kaplan–Meier plot and was calculated using the log-rank test. *$p< 0.05$; **$p<0.01$; and ***$p<0.001$ were considered statistically significant.

Results

AMIGO2 is upregulated in bladder cancer cells and tissues

The result of qRT-PCR showed that the AMIGO2 expression level was elevated in bladder cancer cell lines UMUC3, 5637 and T24 **(Figure 1A).** According to TCGA database, the relative differential expression level (logFC) of AMIGO2 in bladder cancer is also higher than adjacent normal tissue (n=19) **(Figure 1B).** The relative mRNA expression of AMIGO2 in bladder cancer tissues was significantly higher than that of their matched adjacent normal tissues (n=11) **(Figure 1C).** We also found that AMIGO2 expression was up-regulated in bladder cancer tissues compared to the matched adjacent normal tissues by immunohistochemistry (n=43) **(Figure 1D).** Upon clinicopathological correlation analysis,

elevated AMIGO2 is positively correlated with advanced tumor stage (p=0.022) and tumor grade (p=0.041) **(Table 1).**

Table 1 Clinicopathological characteristics of 43 cases with bladder cancer

Variables	Cases	AMIGO2 expression in tumor Number of cases (percentage)		*p*
		Low	High	
Total	43	12	31	
Age				0.775
<65	23	6 (26%)	17 (74%)	
≥65	20	6 (30%)	14 (70%)	
Sex				0.335
Male	36	9 (25%)	27 (75%)	
Female	7	3 (43%)	4 (57%)	
Tumor size				0.521
<3 cm	5	2 (40%)	3 (60%)	
≥3 cm	38	10 (26%)	28 (74%)	
Tumor stage				0.022*
<T2	6	4 (67%)	2 (33%)	
≥T2	37	8 (22%)	29 (78%)	
Tumor grade				0.041*
Low grade	4	3 (75%)	1 (25%)	
High grade	39	10 (26%)	29 (74%)	
Lymph node metastasis				0.633
Negative	19	6 (32%)	13 (68%)	
Positive	24	6 (25%)	18 (75%)	
Vascular invasion				0.791
No	31	9 (29%)	22 (71%)	
Yes	12	3 (25%)	9 (75%)	
Distant metastasis				0.211
No	31	7 (23%)	24 (77%)	
Yes	12	5 (42%)	7 (58%)	

p value was analyzed by a chi-square test; *$p < 0.05$ is considered significant.

AMIGO2 was significantly knocked down in bladder cancer cells

The T24 and 5637 cells stably expressing knockdown AMIGO2 shRNA and negative control shRNA were constructed, selected and expanded. Cells were captured using fluorescent microscope 72 hours after cell transfection **(Figure 2A).** qRT-PCR and WB (Western Blot)

were performed to further evaluate transfection efficiency **(Figure 2B-C).** The results demonstrated that AMIGO2 is knocked down notedly in mRNA level (T24, $p<0.001$; 5637, $p<0.001$), as well as in protein level (T24, $p<0.01$; 5637, $p<0.001$).

Inhibition of AMIGO2 suppresses proliferation and migration, and increases bladder cancer cells chemoresistance in vitro

CCK-8 and wound healing assay showed that suppression of AMIGO2 decreased the proliferation and migration capacity of T24 and 5637 cells in shAMIGO2 group compared with shCtrl group **(Figure 3A-B).** Flow cytometry displayed an increase in the percentage of cells in G1/G0 phase and a decrease in the percentage of cells in S phase **(Figure 3C).** The shAMIGO2 group exhibited a lower suppression ratio than shCtrl group in a series of dilute concentrations of cisplatin **(Figure 3D).** Meanwhile, the IC50 of shAMIGO2 is higher than that of shCtrl (T24, $p=0.002$; 5637, $p=0.004$) **(Figure 3E).** All these results supported that downregulation of AMIGO2 reduces the proliferation and migration and induces G1 phase cell cycle arrest, and that AMIGO2 might reduce chemoresistance to cisplatin in bladder cancer cells.

Inhibition of AMIGO2 reduces tumorigenicity of bladder cancer cells in vivo

The growth of tumors derived from the shAMIGO2 group was prominently suppressed compared with the shCtrl group from 20 days after tumor inoculation (n=5) **(Fig 4A-B).** Also, we detected the expression of AMIGO2 in the xenograft tumors by qRT-PCR. The result showed that the expression level is lower in shAMIGO2 group than that of shCtrl group **(Fig 4C).** These results indicated that inhibition of AMIGO2 reduces bladder cancer cell growth and tumorigenicity in vivo, which was consistent with the in vitro results.

Identification of differentially expressed genes (DEGs) and molecular function and pathway enrichment analysis

As the volcano plots illustrated, after data integration, gene expression profiles from RNA Sequencing identified 917 differentially expressed genes. 627 genes were upregulated and 290 were downregulated in shAMIGO2 compared with the shCtrl in T24 cell **(Figure 5A),**

grounded on the cut-off criteria (|logFC|>2, *P*adj<0.01). DEGs were selected for integrated analysis. We gained the most upregulated 100 genes and 100 downregulated ones to portray the heat map **(Figure 5B),** with red represents high expression level and blue stands for low. In order to investigate the molecular function and biology pathways of the DEGs, GO and KEGG analysis were performed. GO (Gene Ontology) includes molecular function, biological process and cellular component **(Figure 5C-E).** Enriched KEGG pathways of the DEGs are shown in **Figure 5F,** including ABC transporters (ATP-binding cassette transporters), oxytocin signaling pathway, PPAR signaling pathway, etc.

Protein-Protein Interaction (PPI) network construction, hub genes survival analysis and GSEA

The PPI network was constructed based on the SRTING database. A total of 174 proteins were obtained from the DEGs, including 136 nodes and 234 edges **(Figure 6A).** In the network, nodes with top 10 highest degrees were ZAP70, AKR1C1, MAP2K6, SCN2A, AGMAT, CBLB, AKR1C3, TLR3, SCN3A and AZIN2. These genes were considered as hub genes. The information of the 10 hub genes is shown in **Table 2,** including full gene names and primary functions. Total 10 hub genes were obtained from PPI network. The Kaplan-Meier survival analysis **(Figures 6B-E)** shows that four of the 10 hub genes associated with survival were ZAP70, AGMAT, AKR1C1 and AKR1C3. We further explored and verified KEGG pathway on the whole gene expression level by GSEA. The results, as shown in **Figure 6F-G,** displayed two pathways including oxidative phosphorylation and spliceosome.

TABLE 2 Functional roles of the 10 hub genes

No.	Gene	Full name	Function
1	ZAP70	zeta chain of T cell receptor associated protein kinase 70	An enzyme belongs to the PTK family, functions in T-cell development and lymphocyte activation
2	AKR1C1	aldo-keto reductase family 1 member C1	Catalyze the conversion of aldehydes and ketones to their corresponding alcohols
3	MAP2K6	mitogen-activated protein kinase kinase 6	Involved in many cellular processes such as stress induced cell cycle arrest, transcription activation and apoptosis
4	SCN2A	sodium voltage-gated channel alpha subunit 2	Member of the sodium channel alpha subunit gene family
5	AGMAT	agmatinase	Part of an operon in Escherichia coli, constitutes the primary pathway of polyamine synthesis from arginine
6	CBLB	Cbl proto-oncogene B	Encodes an E3 ubiquitin-protein ligase
7	AKR1C3	aldo-keto reductase family 1 member C3	Catalyze the conversion of aldehydes and ketones to their corresponding alcohols
8	TLR3	toll like receptor 3	A member of the Toll-like receptor (TLR) family, functions in pathogen recognition and activation of innate immunity
9	SCN3A	sodium voltage-gated channel alpha subunit 3	Member of the sodium channel alpha subunit gene family
10	AZIN2	antizyme inhibitor 2	The protein belongs to the antizyme inhibitor family, works in cell growth and proliferation

Discussion

Bladder cancer remains to be the most common malignancy in urinary system. Based on the investigations of different genes in malignancies, data are emerging to elucidate gene functions in bladder cancer as well. As is reported before, dysregulation of different genes contributes to certain types of tumor progression. In the present study, we found that AMIGO2 is upregulated in bladder cancer cells and tissues, and it could promote the proliferation, migration and tumorigenicity. AMIGO2 could also reduce chemoresistance to cisplatin in bladder cancer cells. In addition, DEGs, molecular function and pathway enrichment analysis, a PPI network and 10 hub genes were identified using RNA-Seq technology and bioinformatics analysis, which demonstrated the mechanisms of how AMIGO2 regulates BCa cells.

The uncontrolled cell proliferation of cancer is mainly attributed to the cell cycle deregulation[14]. DNA damage targets two cell cycle checkpoints: G1/S and G2/M. DNA damage induces program that blocks cells at one of these checkpoints until the damage is repaired or the cells move towards apoptosis[15]. Arresting cells in G0/G1 phase offers a chance for certain cells to either undergo repairing or tend to apoptosis process. The flow cytometry assay in our study showed that suppression of AMIGO2 could inhibit its proliferative effects through blockage of cell cycle progression and arrest BCa cells in G1 phase. In many cases, an arrest can lead to senescence or apoptosis[16]. Although few studies have described the relationship between AMIGO2 and cell cycle before, there are some pathways that regulate cell cycle indirectly enriched by our KEGG analysis, but the particular pathways and molecules are still under research.

Cisplatin is regarded as cytotoxic drugs, it kills cancer cells by damaging DNA, inhibiting DNA synthesis and mitosis, and inducting apoptotic cell death[17]. Reduced cellular intake, increased efflux and increased DNA repair are thought to be resistance mechanisms to cisplatin in cancer cells[18]. According to our research, AMIGO2 could decrease chemoresistance to cisplatin in BCa cells. Meanwhile, ABC transporters is one of the most essential pathways identified by KEGG pathway enrichment analysis in this study. ABC drug transporters could increase the excretion of their substrate anti-cancer agents, cause decreased intracellular concentration of anti-cancer drugs, and develop the multidrug resistance (MDR) phenotype[19]. Previous studies showed that ATP-binding cassette subfamily B member 1 (ABCB1) is also known as multidrug resistance protein 1 or P-glycoprotein; ABCC1 is considered as multidrug resistance associated protein 1, and ABCG2 is regarded as a breast cancer resistance protein[20]. When these ABC-transporter pumps are upregulated, substrates of drugs would be actively excreted from cancer cells, resulting in decreased intracellular drug accumulation. This might be one of the explanations that how AMIGO2 functions in reducing chemoresistance.

GO term enrichment analysis showed that the DGEs were significantly enriched in extracellular matrix, lipid transporter activity and cell-cell adhesion via plasma-membrane adhesion molecules, suggesting that some of these DEGs might be involved in cell adhesion and migration. As stated in previous studies, PCDH1 mediated cell-cell adhesion through homotypic interactions[21], CELSR1 regulated endothelial adherens junctions and directed cell rearrangements during valve morphogenesis[22], and PCDHGA3 worked as one of the cell adhesion molecules in human ischemic cardiomyopathy[23]. Cell adhesion participants in stimulating signals that regulate cell cycle, migration, and cell survival[24]. Cell adhesiveness is generally reduced in different kinds of human cancers. AMIGO2, as reported before, is also involved in cell adhesion and/or cell migration[6,25,26]. Changes of these molecules might be leading to the reduction of adhesion between cells and promoting the migration of tumor cells. Meanwhile, the wound healing assay in this study also proved that AMIGO2 could promote the migration of BCa cells.

Finally, we explored the interaction of DEGs. As a result, a large and complex interactome network was established, suggesting intricate links among those DEGs. Moreover, 10 hub genes were identified in total, 4 of them were related to survival, namely ZAP70, AGMAT, AKR1C1 and AKR1C3. Studies have shown that ZAP70 is involved in the development of chronic lymphocytic leukemia[27]. AGMAT could promote the lung adenocarcinoma tumorigenesis by activating the NO-MAPKs-PI3K/ Akt pathway[28]. Interestingly, as previous studies stated, AKR1C1 could mediate the invasive potential and drug resistance of metastatic bladder cancer cells, and AKR1C1 was highly expressed in metastatic lesions of human bladder cancer patients[29]. AKR1C3, comes from the same family as AKR1C1, has not been proved to have similar functions as AKR1C1 in bladder cancer, but it is often overexpressed in prostate cancer tissues and prostate cancer cell lines[30]. AKR1C3 catalyzes the formation of prostaglandin (PG) F2α and 11β-PGF2α from PGH2 and PGD2, respectively[31]. The PGF2α and 11β-PGF2α can inactivate peroxisome proliferator-activated receptor gamma (PPAR-γ) and has anti-proliferative effects[32]. Coincidentally, PPAR

is one of the pathways enriched by KEGG analysis in our study, but the exact relationships and functions remain elusive.

To the best of our knowledge, this is the first study determining the very “new” gene AMIGO2, which promotes the proliferation, migration and tumorigenicity in BCa. In addition, AMIGO2 could reduce chemoresistance to cisplatin. Some DEGs were identified to be related to cell-cell adhesion. Certain pathways were recognized to be involved in tumor development or drug resistance. Whereas, the molecules and pathways identified by bioinformatics analysis have not been examined by our research yet. Therefore, exploring molecular functions of DEGs and verifying pathways that are regulated by AMIGO2 would be our next-step work.

Conclusion

AMIGO2 is overexpressed in bladder cancer cells and tissues and serves as an oncogene in bladder cancer. It also reduces chemoresistance to cisplatin. The process might be regulated by the identified DEGs and particular pathways including ABC transporters and PPAR signaling pathway. Four hub genes might be associated with prognosis of bladder cancer patients. The study provided a potential therapeutic target and underlying mechanisms for BCa treatment. Nevertheless, the identified DEGs and pathways still need to be further confirmed by additional relevant studies.

Declarations

- Ethics approval and consent to participate

All tissue samples were obtained from patients who have signed informed consent. This project was approved by the Institutional Research Ethics Committee of the Second Hospital of Lanzhou University (Approval No. 2019A-199).

All mouse experiments were conducted with standard operating procedures approved by the University Committee on the Use and Care of Animals at the second hospital of Lanzhou University (Approval No. D2019-171).

- Consent for publication

Not applicable.

- Availability of data and materials

The datasets generated and/or analysed during the current study are available in the TCGA repository [https://www.cancer.gov/about-nci/organization/ccg/research/structural-genomics/tcga] and Genebank [https://cipotato.org/genebankcip/]

The datasets used and/or analysed during the current study are available from the corresponding author on reasonable request.

All data generated or analysed during this study are included in this published article [and its supplementary information files].

- Competing interests

The authors declare that they have no competing interests.

- Funding

This study was supported by the Science and Technology project of Chengguan District, Lanzhou city, Gansu province Science and Technology Bureau (Project number: 2017KJGG0052), the Cuiying Graduate Supervisor Applicant Training Program of Lanzhou University Second Hospital (201704), the Gansu Health Industry Research Project (GSWSKY2017-10), the Cuiying Scientific and Technological Innovation Program of Lanzhou University Second Hospital (Project number: CY2017-BJ16, Doctoral supervisor training program), and the National Nature Science Foundation of China (NO: 81372732&30800206). There was no additional external funding received for this study. The funders had no role in study design, data collection and analysis, decision to publish, or preparation of the manuscript.

- Authors' contributions

J.-q.T. conceived and designed the experiments. D.-l.H., X.-x.Z., C.-h.C., Z.-q.Y. and H.W. performed the experiments and analyzed the data. B.X., J.-l.C., J.-p.L. and P.L. did bioinformatics analysis and provided statistical support. D.-l.H. prepared the manuscript. Z.-p.W. helped write the manuscript. All authors read and approved the final manuscript.

- Acknowledgements

Not applicable.

- Authors' information (optional)

References

1 Bray, F., Ferlay, J., Soerjomataram, I., Siegel, R. L., Torre, L. A. & Jemal, A. **Global cancer statistics 2018: GLOBOCAN estimates of incidence and mortality worldwide for 36 cancers in 185 countries**. *CA Cancer J Clin* 2018 **68**, 394-424, doi:10.3322/caac.21492.

2 Cancer Genome Atlas Research, N. **Comprehensive molecular characterization of urothelial bladder carcinoma**. *Nature* 2014 **507**, 315-322, doi:10.1038/nature12965.

3 Boehm, B. E. & Svatek, R. S. **Novel Therapeutic Approaches for Recurrent Nonmuscle Invasive Bladder Cancer**. *Urologic Clinics of North America* 2015 **42**, 159-168, doi:10.1016/j.ucl.2015.02.001.

4 Genebank. https://cipotato.org/genebankcip/. Accessed 18 Jan 2020.

5 Kuja-Panula, J., Kiiltomäki, M., Yamashiro, T., Rouhiainen, A. & Rauvala, H. **AMIGO, a transmembrane protein implicated in axon tract development, defines a novel protein family with leucine-rich repeats**. *The Journal of Cell Biology* 2003 **160**, 963-973, doi:10.1083/jcb.200209074.

6 Rabenau, K. E., O'Toole, J. M., Bassi, R., Kotanides, H., Witte, L., Ludwig, D. L. & Pereira, D. S. **DEGA/AMIGO-2, a leucine-rich repeat family member, differentially expressed in human gastric adenocarcinoma: effects on ploidy, chromosomal stability, cell adhesion/migration and tumorigenicity**. *Oncogene* 2004 **23**, 5056-5067, doi:10.1038/sj.onc.1207681.

7 Fontanals-Cirera, B., Hasson, D., Vardabasso, C., Di Micco, R., Agrawal, P., Chowdhury, A., Gantz, M., de Pablos-Aragoneses, A., Morgenstern, A., Wu, P., Filipescu, D., Valle-Garcia, D., Darvishian, F., Roe, J. S., Davies, M. A., Vakoc, C. R., Hernando, E. & Bernstein, E. **Harnessing BET Inhibitor Sensitivity Reveals AMIGO2 as a Melanoma Survival Gene**. *Mol Cell* 2017 **68**, 731-744 e739, doi:10.1016/j.molcel.2017.11.004.

8 Wang, B., Xu, D., Yu, X., Ding, T., Rao, H., Zhan, Y., Zheng, L. & Li, L. **Association of intra-tumoral infiltrating macrophages and regulatory T cells is an independent prognostic factor in gastric cancer after radical resection**. *Ann Surg Oncol* 2011 **18**, 2585-2593, doi:10.1245/s10434-011-1609-3.

9 Schmittgen, T. D. & Livak, K. J. **Analyzing real-time PCR data by the comparative CT method**. *Nature Protocols* 2008 **3**, 1101-1108, doi:10.1038/nprot.2008.73.

10 Sebaugh, J. L. **Guidelines for accurate EC50/IC50 estimation**. *Pharm Stat* 2011 **10**, 128-134, doi:10.1002/pst.426.

11 Cumashi, A., Tinari, N., Rossi, C., Lattanzio, R., Natoli, C., Piantelli, M. & Iacobelli, S. **Sunitinib malate (SU-11248) alone or in combination with low-dose docetaxel inhibits the growth of DU-145 prostate cancer xenografts**. *Cancer Lett* 2008 **270**, 229-233, doi:10.1016/j.canlet.2008.05.007.

12 Yang, Z., Liang, X., Fu, Y., Liu, Y., Zheng, L., Liu, F., Li, T., Yin, X., Qiao, X. & Xu, X. **Identification of AUNIP as a candidate diagnostic and prognostic biomarker for oral squamous cell carcinoma**. *EBioMedicine* 2019 **47**, 44-57, doi:10.1016/j.ebiom.2019.08.013.

13 The Cancer Genome Atlas Program. https://www.cancer.gov/about-nci/organization/ccg/research/structural-genomics/tcga. 19 Nov 2019.

14 Malumbres, M. & Barbacid, M. **Cell cycle, CDKs and cancer: a changing paradigm**. *Nature Reviews Cancer* 2009 **9**, 153-166, doi:10.1038/nrc2602.

15 Sitko, J. C., Yeh, B., Kim, M., Zhou, H., Takaesu, G., Yoshimura, A., McBride, W. H., Jewett, A., Jamieson, C. A. & Cacalano, N. A. **SOCS3 regulates p21 expression and cell cycle arrest in response to DNA damage**. *Cell Signal* 2008 **20**, 2221-2230, doi:10.1016/j.cellsig.2008.08.011.

16 Lagunas-Cruz, M. D. C., Valle-Mendiola, A., Trejo-Huerta, J., Rocha-Zavaleta, L., Mora-Garcia, M. L., Gutierrez-Hoya, A., Weiss-Steider, B. & Soto-Cruz, I. **IL-2 Induces Transient Arrest in the G1 Phase to Protect Cervical Cancer Cells from Entering Apoptosis**. *J Oncol* 2019 **2019**, 7475295, doi:10.1155/2019/7475295.

17 Dasari, S. & Tchounwou, P. B. **Cisplatin in cancer therapy: molecular mechanisms of action**. *Eur J Pharmacol* 2014 **740**, 364-378, doi:10.1016/j.ejphar.2014.07.025.

18 Holohan, C., Van Schaeybroeck, S., Longley, D. B. & Johnston, P. G. **Cancer drug resistance: an evolving paradigm**. *Nature Reviews Cancer* 2013 **13**, 714, doi:10.1038/nrc3599.

19 Anreddy, N., Gupta, P., Kathawala, R. J., Patel, A., Wurpel, J. N. & Chen, Z. S. **Tyrosine kinase inhibitors as reversal agents for ABC transporter mediated drug resistance**. *Molecules* 2014 **19**, 13848-13877, doi:10.3390/molecules190913848.

20 Robey, R. W., Pluchino, K. M., Hall, M. D., Fojo, A. T., Bates, S. E. & Gottesman, M. M. **Revisiting the role of ABC transporters in multidrug-resistant cancer**. *Nat Rev Cancer* 2018 **18**, 452-464, doi:10.1038/s41568-018-0005-8.

21 Faura Tellez, G., Willemse, B. W., Brouwer, U., Nijboer-Brinksma, S., Vandepoele, K., Noordhoek, J. A., Heijink, I., de Vries, M., Smithers, N. P., Postma, D. S., Timens, W., Wiffen, L., van Roy, F., Holloway, J. W., Lackie, P. M., Nawijn, M. C. & Koppelman, G. H. **Protocadherin-1 Localization and Cell-Adhesion Function in Airway Epithelial Cells in Asthma**. *PLoS One* 2016 **11**, e0163967, doi:10.1371/journal.pone.0163967.

22 Tatin, F., Taddei, A., Weston, A., Fuchs, E., Devenport, D., Tissir, F. & Makinen, T. **Planar cell polarity protein Celsr1 regulates endothelial adherens junctions and directed cell rearrangements during valve morphogenesis**. *Dev Cell* 2013 **26**, 31-44, doi:10.1016/j.devcel.2013.05.015.

23 Ortega, A., Gil-Cayuela, C., Tarazon, E., Garcia-Manzanares, M., Montero, J. A., Cinca, J., Portoles, M., Rivera, M. & Rosello-Lleti, E. **New Cell Adhesion Molecules in Human Ischemic Cardiomyopathy. PCDHGA3 Implications in Decreased Stroke Volume and Ventricular Dysfunction**. *PLoS One* 2016 **11**, e0160168, doi:10.1371/journal.pone.0160168.

24 Huang, S. & Ingber, D. E. **The structural and mechanical complexity of cell-growth control**. *Nature Cell Biology* 1999 **1**, E131-E138, doi:10.1038/13043.

25 Kanda, Y., Osaki, M., Onuma, K., Sonoda, A., Kobayashi, M., Hamada, J., Nicolson, G. L., Ochiya, T. & Okada, F. **Amigo2-upregulation in Tumour Cells Facilitates Their Attachment to Liver Endothelial Cells Resulting in Liver Metastases**. *Sci Rep* 2017 **7**, 43567, doi:10.1038/srep43567.

26 Chen, J., Gu, L., Ni, J., Hu, P., Hu, K. & Shi, Y. L. **MiR-183 Regulates ITGB1P Expression and Promotes Invasion of Endometrial Stromal Cells**. *Biomed Res Int* 2015 **2015**, 340218, doi:10.1155/2015/340218.

27 Carabia, J., Carpio, C., Abrisqueta, P., Jimenez, I., Purroy, N., Calpe, E., Palacio, C., Bosch, F. & Crespo, M. **Microenvironment regulates the expression of miR-21 and tumor suppressor genes PTEN, PIAS3 and PDCD4 through ZAP-70 in chronic lymphocytic leukemia**. *Sci Rep* 2017 **7**, 12262, doi:10.1038/s41598-017-12135-7.

28 Zhu, H. E., Yin, J. Y., Chen, D. X., He, S. & Chen, H. **Agmatinase promotes the lung adenocarcinoma tumorigenesis by activating the NO-MAPKs-PI3K/Akt pathway**. *Cell Death Dis* 2019 **10**, 854, doi:10.1038/s41419-019-2082-3.

29 Matsumoto, R., Tsuda, M., Yoshida, K., Tanino, M., Kimura, T., Nishihara, H., Abe, T., Shinohara, N., Nonomura, K. & Tanaka, S. **Aldo-keto reductase 1C1 induced by interleukin-1beta mediates the invasive potential and drug resistance of metastatic bladder cancer cells**. *Sci Rep* 2016 **6**, 34625, doi:10.1038/srep34625.

30 Doig, C. L., Battaglia, S., Khanim, F. L., Bunce, C. M. & Campbell, M. J. **Knockdown of AKR1C3 exposes a potential epigenetic susceptibility in prostate cancer cells**. *J Steroid Biochem Mol Biol* 2016 **155**, 47-55, doi:10.1016/j.jsbmb.2015.09.037.

31 Liu, C., Yang, J. C., Armstrong, C. M., Lou, W., Liu, L., Qiu, X., Zou, B., Lombard, A. P., D'Abronzo, L. S., Evans, C. P. & Gao, A. C. **AKR1C3 Promotes AR-V7 Protein Stabilization and Confers Resistance to AR-Targeted Therapies in Advanced Prostate Cancer**. *Mol Cancer Ther* 2019 **18**, 1875-1886, doi:10.1158/1535-7163.MCT-18-1322.

32 Julian, C. D. e. a. **The aldo-keto reductase AKR1C3 is a novel suppressor of cell differentiation that provides a plausible target for the non-cyclooxygenase-dependent antineoplastic actions of nonsteroidal anti-inflammatory drugs**. *Cancer Res* 2003 **63**, 505-512.

Figures

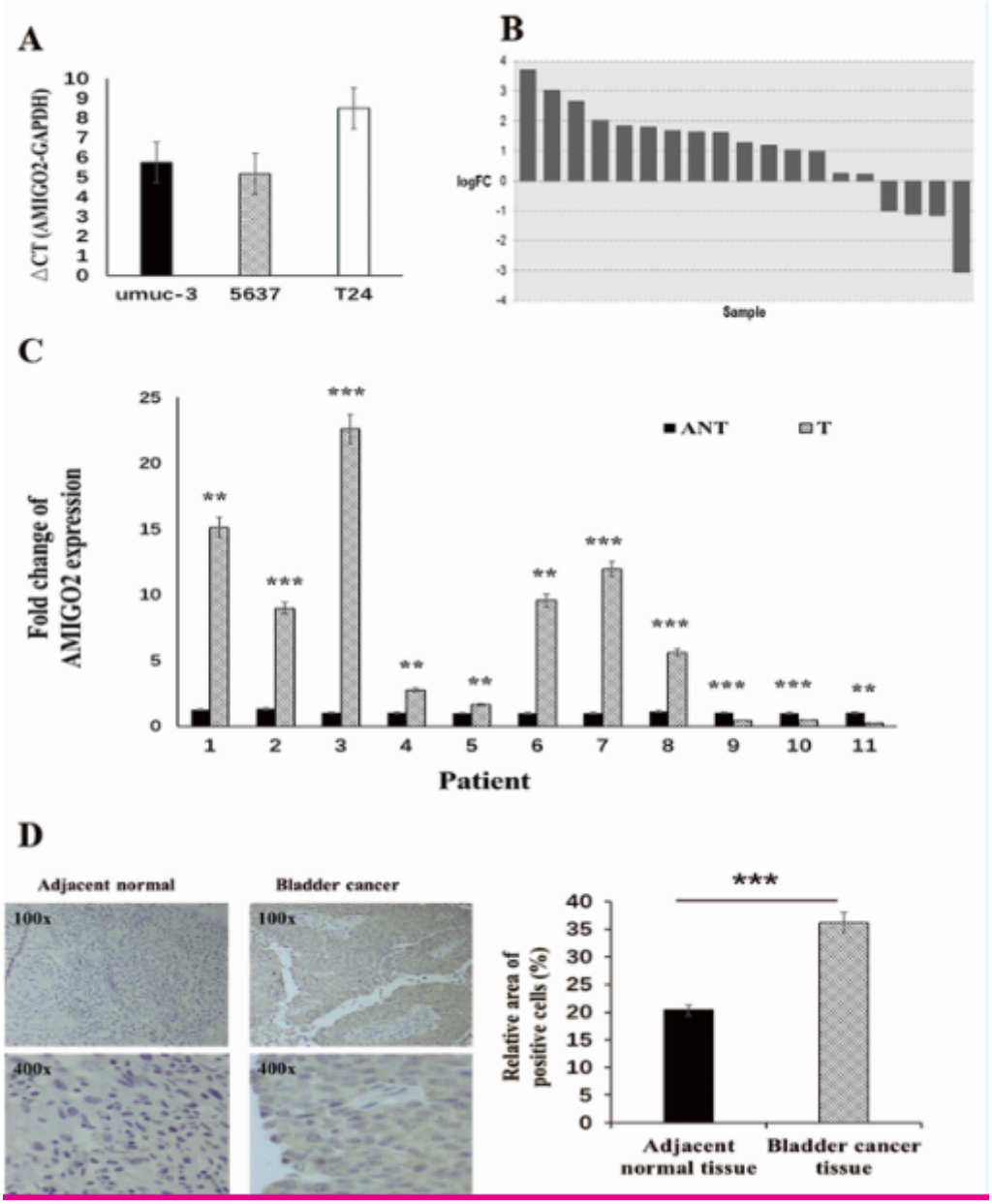

Figure 1

A. qRT-PCR analysis of AMIGO2 expression in bladder cancer cell lines, UMUC3, 5637 and T24 (95% confidence interval, 4.50-6.98, 4.71-5.59, 8.06-8.90, respectively). B. TCGA database analysis13 of the relatively differential expression level (logFC) of AMIGO2 in bladder cancer tissues and adjacent normal tissues (n=19). C. The expression of AMIGO2 was examined in cancerous tissues (T) and their adjacent non-cancerous bladder tissues (ANT) (n=11, 95% CI, ANT: 1.00-1.15, T: 2.35-12.07). D. Representative IHC images of AMIGO2 expression in BCa tissues and the corresponding adjacent normal bladder tissues (n=43). All images were captured at 100× and 400× magnification. Data were based on at least three independent experiments, and shown as mean ± SEM (*p< 0.05, **p< 0.01, ***p< 0.001).

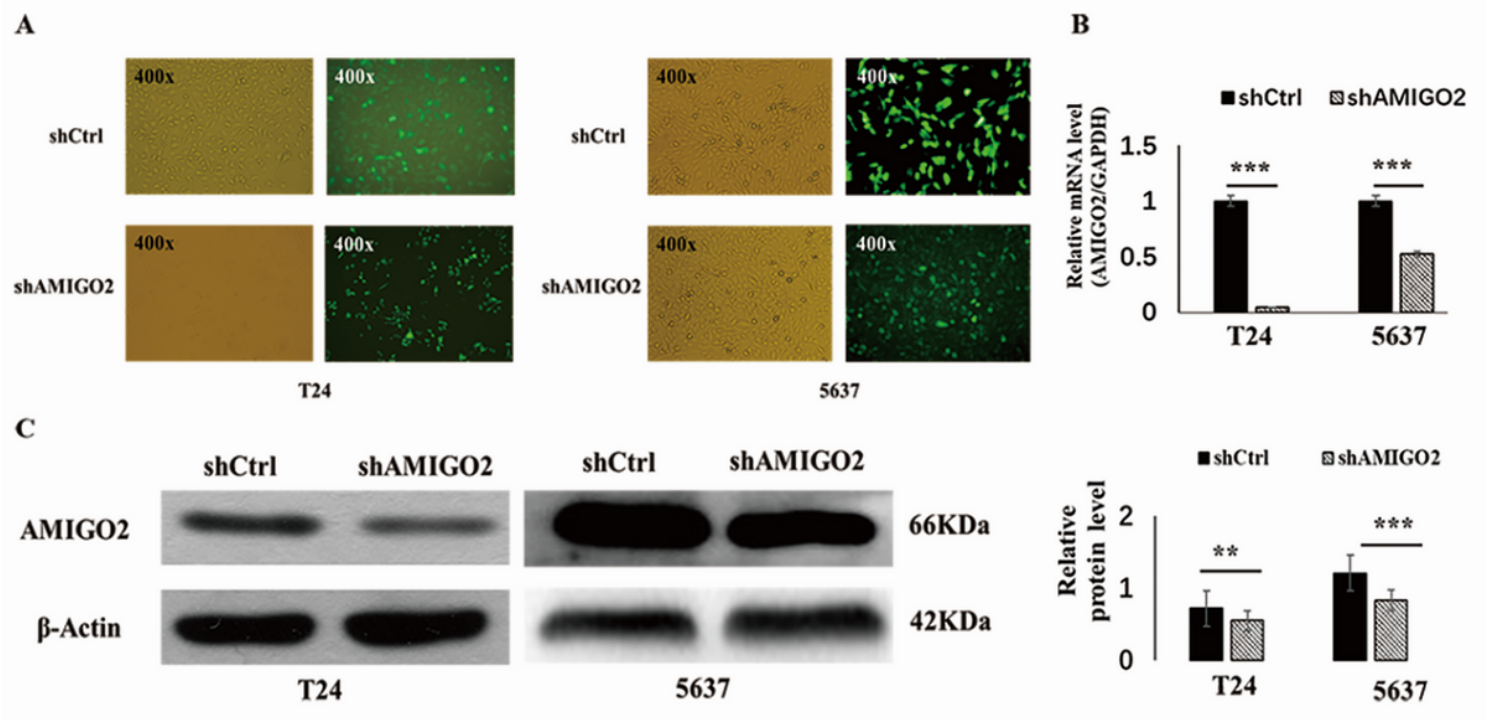

Figure 2

A. shAMIGO2 and shCtrl cells were captured using fluorescent microscope 72 hours after cell transfection. B. the relative mRNA expression level of AMIGO2 after cell transfection. C. Western blot was used for detection of protein expression level of AMIGO2 after cell transfection. Three independent experiments yielded similar results. The results are presented as the means ± SEM of values obtained in three independent experiments. Statistical significance was calculated using the Student's t-tests. *p < 0.05, **p< 0.01, ***p< 0.001.

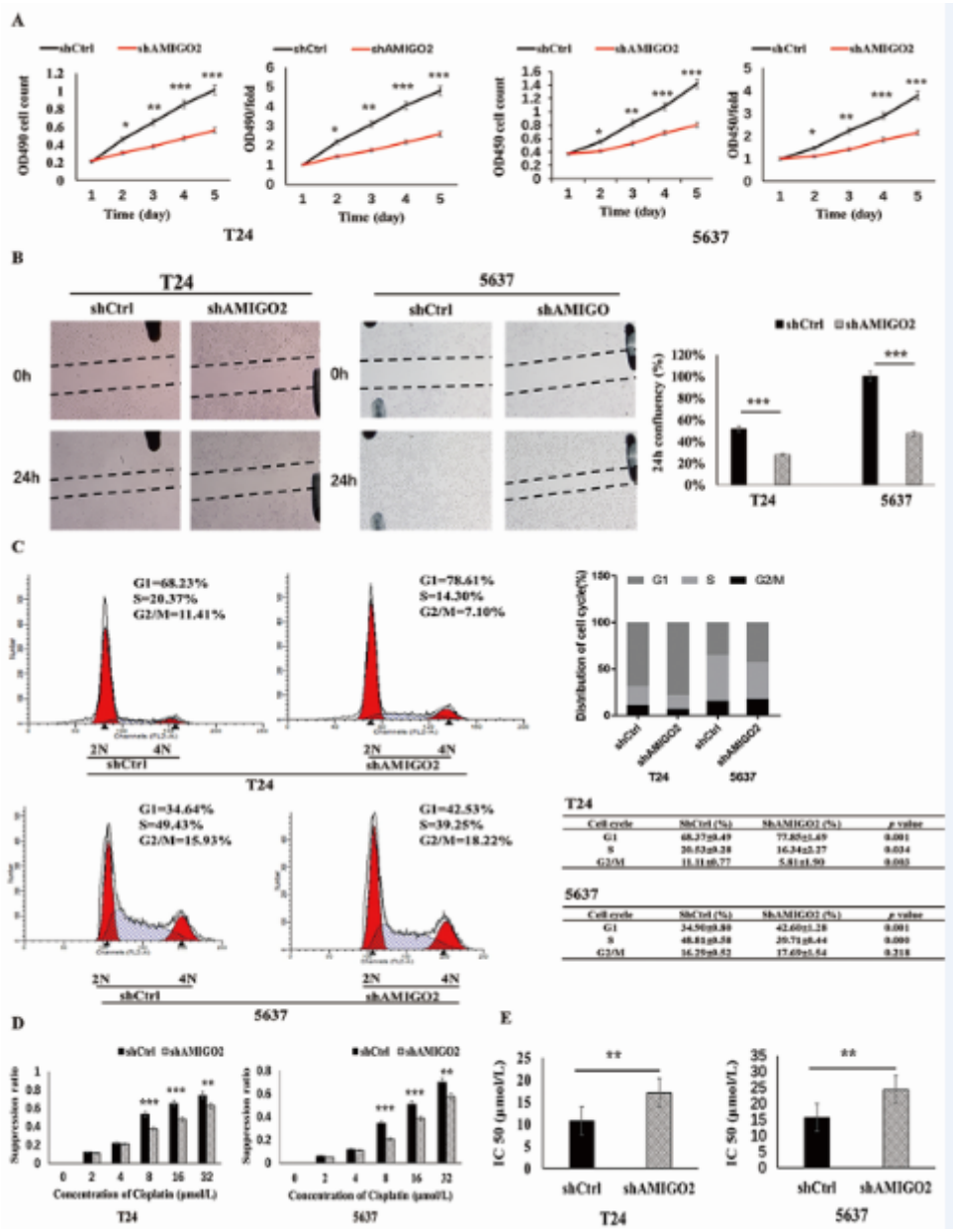

Figure 3

A. Effects of shAMIGO2 and shCtrl on the proliferation of bladder cancer cell lines T24 and 5637, detected by CCK-8. B. Effects of shAMIGO2 and shCtrl on the migration BCa cells, assessed by wound healing assay. C. Effects of shAMIGO2 and shCtrl on cell cycle of the indicated cells, analyzed by flow cytometry. D. Cells were treated with cisplatin for 24h, and then analyzed by CCK-8 assay. The suppression ratio of shAMIGO2 group is lower than shCtrl group. E. Transfection of shAMIGO2 decreased the sensitivity to cisplatin. For calculation of IC50, four parameter logistic curve (best-fit solution, nonlinear regressiondynamic fitting) and normality tests are used (Graph Pad Prism 5). Bars represent the mean ± SEM of three independent experiments. *p< 0.05, **p< 0.01, ***p< 0.001.

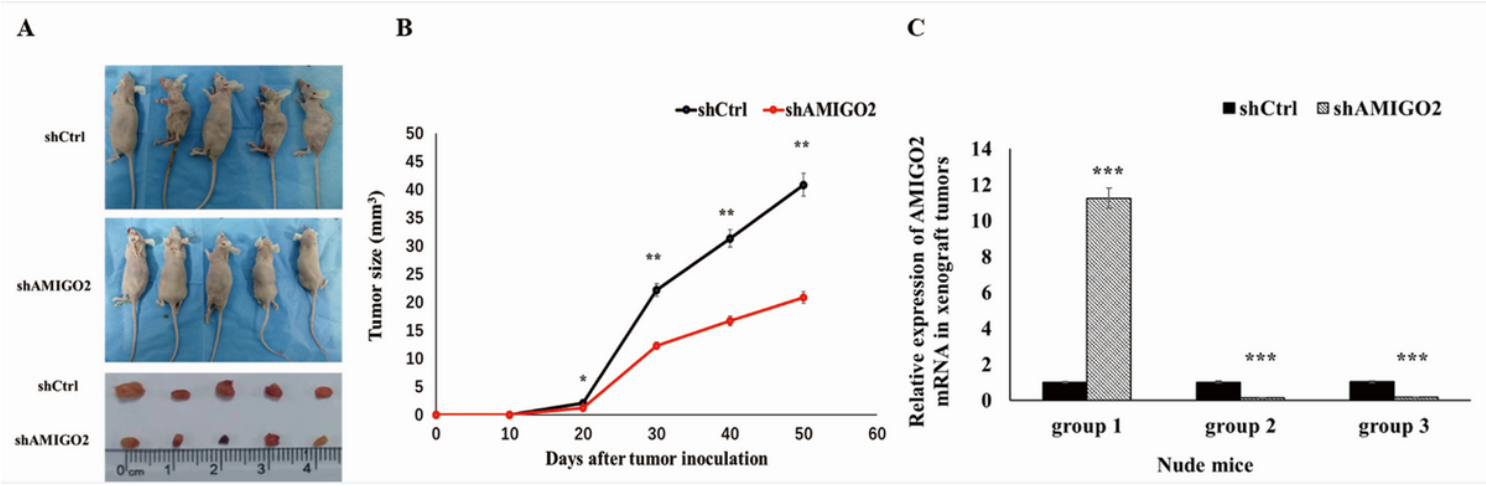

Figure 4

AMIGO2 promotes tumorigenicity of bladder cancer cells in vivo. A. The image of animals and tumors. B. The volume of tumors, detected for 50 days. The results are presented as the means ± SEM of values (n=5) (95% CI, 20d, shCtrl: -0.08-3.20, shAMIGO2: -0.77-3.27; 30d, shCtrl: 4.00-47.48, shAMIGO2: 3.79-20.78; 40d, shCtrl: 9.12-53.58, shAMIGO2: 5.49-27.95; 50d, shCtrl: 7.17-74.55, shAMIGO2: 9.67-32.08). C. The expression of AMIGO2 was detected in the xenograft tumors by qRT-PCR. Statistical significance was calculated using the Student's t-tests. Data were based on at least three independent experiments, and shown as mean ± SEM (*p< 0.05, **p< 0.01, ***p< 0.001).

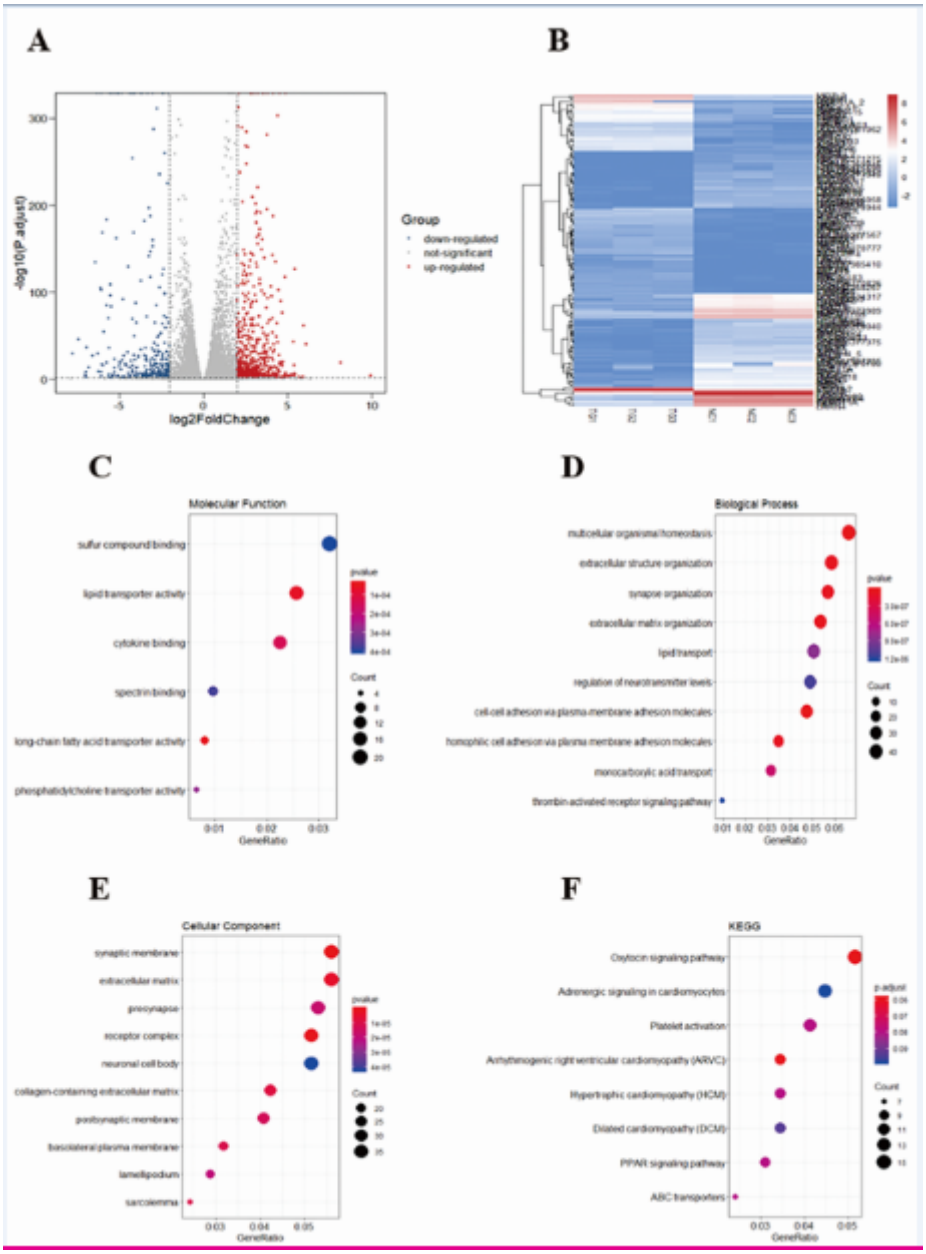

Figure 5

A. Identification of differentially expressed genes. Volcano plot of gene expression profiles. Red/blue symbols classify the upregulated/downregulated genes according to the criteria: |logFC|>2 and adjusted p-value<0.01. B. The heat map shows the differential gene expression profiles of shAMIGO2 group in comparison with shCtrl group. Blue, red and white respectively represents a lower expression level, a higher expression level and no expression difference among the genes. C. Molecular function, which were significantly enriched in lipid transporter activity, cytokine binding and long-chain fatty acid transporter activity; D. Biological process, which were significantly enriched in multicellular organismal homeostasis, extracellular structure organization and synapse organization; E. Cellular component, which were significantly enriched in synaptic membrane, extracellular matrix and receptor complex. F. KEGG pathways in which DEGs were significantly enriched. There were 8 pathways in the relation graph, including oxytocin signaling pathway, adrenergic signaling in cardiomyocytes, platelet activation, ARVC,

HCM, DCM, PPAR signaling pathway and ABC transporters. Size of the dots: Count of DEGs enriched in corresponding GO and KEGG classification.

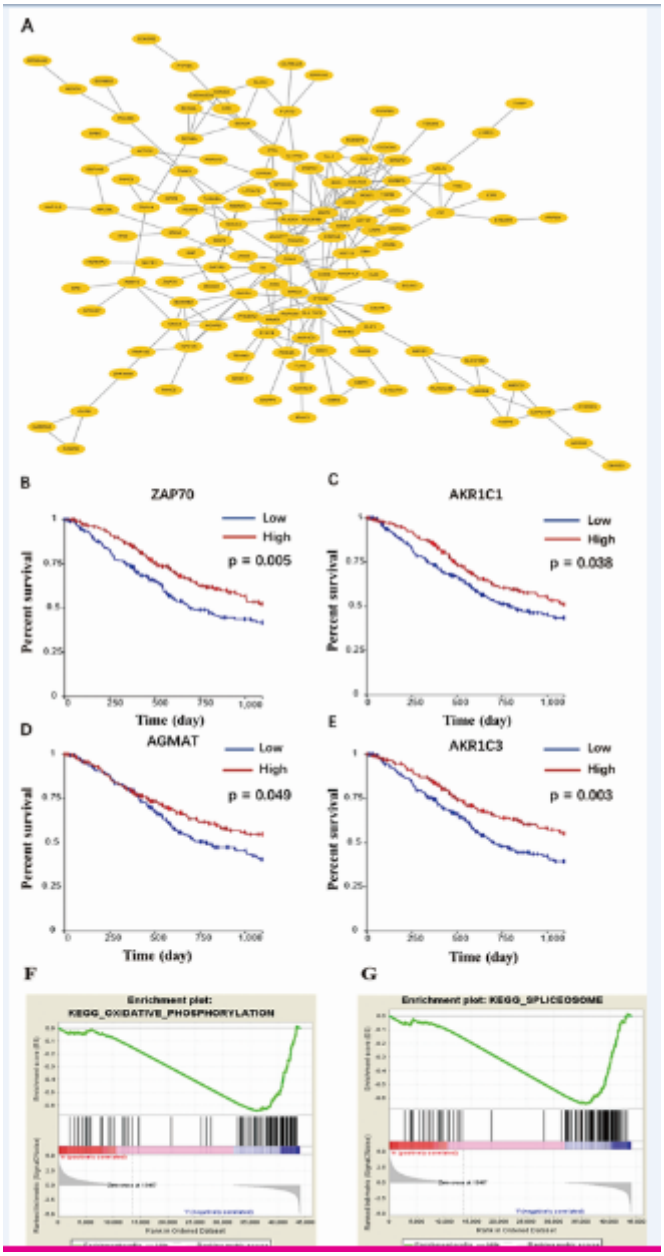

Figure 6

A. Modules with relatively high score selected from the protein-protein interaction network. The PPI network contains 136 nodes and 234 edges. ZAP70, AKR1C1, MAP2K6, SCN2A, AGMAT, CBLB, AKR1C3, TLR3, SCN3A and AZIN2 were considered as hub genes. B-E. Four genes significantly related to survival. The red line indicates the group with higher expression of this gene, and the blue line indicates the group with lower expression. F-G. The two enrichment plots from the GSEA results, namely oxidative phosphorylation (p = 0.000, FDR = 0.685) and spliceosome (p = 0.000, FDR = 0.532).